Blind instrument response function identification from fluorescence decays

Adrián Gómez-Sánchez,[1,2,*] Olivier Devos,[2] Raffaele Vitale,[2] Michel Sliwa,[2] Damir Sakhapov,[3] Jörg Enderlein,[3] Anna de Juan,[1] and Cyril Ruckebusch[2]

[1]Chemometrics Group, Universitat de Barcelona, Barcelona, Spain; [2]Université Lille, CNRS, UMR 8516, Laboratoire Avancé de Spectroscopie pourles Intéractions la Réactivité et l'Environnement (LASIRE), Lille, France; and [3]III. Institute of Physics – Biophysics, Georg-August Universität, Göttingen, Germany

ABSTRACT   Time-resolved fluorescence spectroscopy plays a crucial role when studying dynamic properties of complex photochemical systems. Nevertheless, the analysis of measured time decays and the extraction of exponential lifetimes often requires either the experimental assessment or the modeling of the instrument response function (IRF). However, the intrinsic nature of the IRF in the measurement process, which may vary across measurements due to chemical and instrumental factors, jeopardizes the results obtained by reconvolution approaches. In this paper, we introduce a novel methodology, called blind instrument response function identification (BIRFI), which enables the direct estimation of the IRF from the collected data. It capitalizes on the properties of single exponential signals to transform a deconvolution problem into a well-posed system identification problem. To delve into the specifics, we provide a step-by-step description of the BIRFI method and a protocol for its application to fluorescence decays. The performance of BIRFI is evaluated using simulated and time-correlated single-photon counting data. Our results demonstrate that the BIRFI methodology allows an accurate recovery of the IRF, yielding comparable or even superior results compared with those obtained with experimental IRFs when they are used for reconvolution by parametric model fitting.

WHY IT MATTERS   Time-resolved fluorescence spectroscopy is a crucial tool for understanding dynamic processes in photochemical systems. However, the interference of the instrument response function (IRF) complicates accurate analysis. The novel blind instrument response function identification (BIRFI) methodology proposed in this paper addresses this challenge. BIRFI transforms the deconvolution problem into a well-posed system identification problem, allowing the direct estimation of the IRF from measurements on fluorophores exhibiting single exponential behavior. This innovation is particularly significant since it suppresses the need to estimate the IRF through specific experimental procedures involving fluorophores with very short lifetimes or detectors that may suffer from color effects.

INTRODUCTION

Time-resolved fluorescence spectroscopy (TRFS) is a widely used tool to investigate the dynamic properties of complex photochemical systems (1,2). A short laser pulse is employed to initiate the excitation of fluorescent molecules within a complex sample. The subsequent return of these molecules to the ground state generates a fluorescence signal, denoted as x, which diminishes over time. Ideally, this signal can be fitted by a mono- or multiexponential model, enabling the extraction of the lifetime(s) and amplitude(s) of the fluorescent species involved.

However, the detection of rapidly decaying responses that might be observable in a particular experiment is hindered by the instrument response function (IRF). This complication arises due to the interference of the IRF with the fluorescence signal, especially in scenarios where fast dynamics are at play (3). TRFS measurements can be accurately characterized as the convolution of the IRF with the inherent fluorescence signal x. In other words, the recorded signal, denoted as y, can be expressed analytically as detailed in Eq. 1.

$$y = x * \mathrm{IRF} \qquad \text{(Equation 1)}$$

where * denotes functional convolution.

In the realm of discrete time signals, operators and practitioners may encounter the need to: 1) compute x based on y and the IRF through deconvolution (4), 2) determine the IRF based on y and x using system identification (5), or 3) simultaneously estimate both x and the IRF given y through blind deconvolution (4). Each of these can pose challenges, since it is often ill-posed and not easily solved. To address these complexities, additional constraints, assumptions, or prior knowledge about the signals and systems under investigation must frequently be considered.

In TRFS, deconvolution is a standard operation since, when dealing with short lifetimes, typically around or below 1 ns, it requires knowledge or experimental estimation of the IRF. In the literature, experimental estimation of the IRF often involves measuring the emission of a fluorophore with a very short fluorescence lifetime, such as Erythrosine B or Rose Bengal in a potassium iodide solution (6,7), or the elastic scattering of the excitation laser pulse using a LUDOX solution (3). Once the IRF is estimated, deconvolution of the measured signal y can be performed, enabling the estimation of the true signal x. Various approaches can be employed for this purpose, including polynomial long division (8), least squares (9), Fourier deconvolution (9), and reconvolution (10). Reconvolution is a parametric fitting approach, where, given a specific IRF, Eq. 1 is least squares fitted to estimate the parameters of a mono- or multiexponential model that describes the behavior of x. This method is widely used due to its numerical stability, but it does have several limitations (11,12).

One significant limitation is the intrinsic variability of the IRF, which may change across measurements due to chemical and instrumental factors. For example, TRFS measurements are often "emission dependent," in part because of the wavelength-dependent timing response of certain detectors (such as Micro Photon Devices, single photon avalanche photodiodes). In this case, the measured IRF is only strictly valid for wavelength ranges that are close to those used for the IRF estimation, specifically the laser wavelength for scattering or dye emission. This dependence is particularly noticeable in the red region of the electromagnetic spectrum, crucial for biological imaging (13). This leads to potential biases in the extraction of x when the measured IRF is used for reconvolution and parameter estimation. Various solutions have been suggested to address this issue, including the implementation of detectors robust to color effects or the utilization of a single exponential decay for correcting the phasor plot domain (14,15).

Additional limitations stem from the signal processing methods employed for deconvolution. Optimization algorithms like the Levenberg-Marquardt algorithm, commonly used in reconvolution, can be sensitive to local minima (9). Furthermore, approaches like polynomial long division or Fourier transform are known to be highly sensitive to noise (9).

In contrast, system identification is a relatively straightforward scenario when x is known and the IRF signal comprises fewer sampling points than y. In such instances, convolution can be expressed as an overdetermined system of linear equations (more equations than unknowns) by utilizing a Hankel matrix composed of corresponding shifted values of x (16). Consequently, an ordinary least-squares solution to this system of equations can always be found, as long as the Hankel matrix is invertible.

Blind deconvolution, on the other hand, often proves to be a challenging and critical process. It involves the simultaneous estimation of both the IRF and x, presenting an ill-posed and underdetermined problem (4). This essentially implies that the solution for x and IRF is not unique.

In TRFS data analysis, although the IRF is typically much shorter than the measured signal, practical application of system identification is rare. This is primarily due to the requirement of the knowledge of the underlying signal x, which is generally unavailable. However, if x exhibit a single exponential decay behavior, the IRF can be extracted solely from the analysis of the measured signal y, since its tail behaves as x, up to scale variations. This is what blind instrument response function identification (BIRFI), the new algorithm proposed in this paper, can achieve by leveraging the properties of exponential signals. BIRFI overcomes the main limitations of current methods, such as those related to potential color effects of detectors or the necessity to use specific fluorophores with very short lifetimes. Therefore, BIRFI provides the researchers with the possibility to extract the IRF from measurements carried out on affordable commercial fluorophores under experimental conditions that match the characteristics of their samples. Once the IRF is extracted, it can also be exploited for the analysis of unknown samples.

We provide a comprehensive, step-by-step description of BIRFI and its specific application to fluorescence decays. To gauge its efficacy, we rigorously assess its performance using simulated data and real time-correlated single-photon counting (TCSPC) data sets representative of diverse analytical scenarios, specifically in the red emission range and using a common picosecond diode laser with IRF-dependent power.
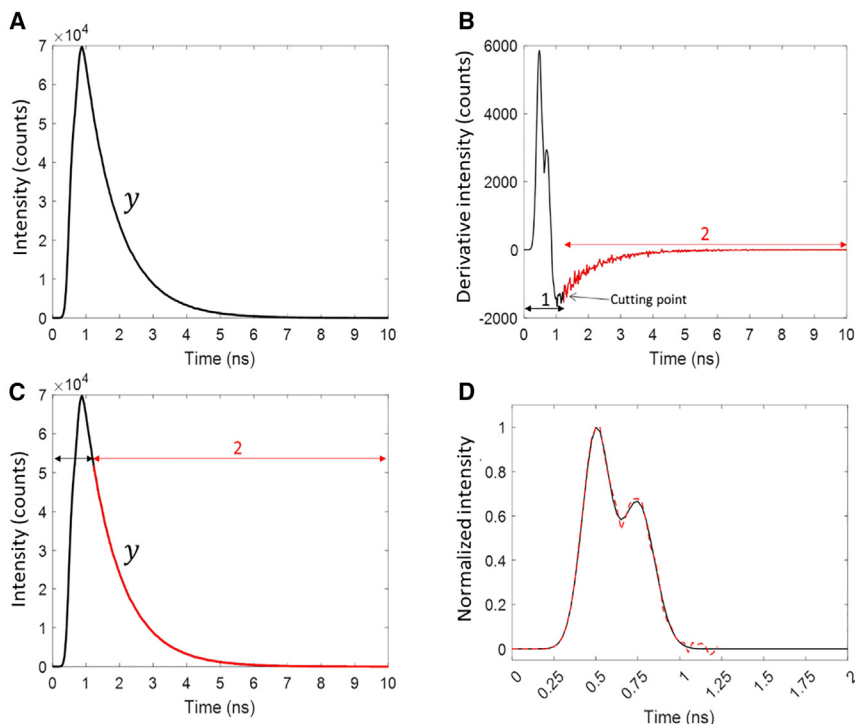
FIGURE 1 (*A*) Measured convolved decay *y*. (*B*) Derivative of the measured convolved decay featuring an initial nonexponential trend (*black*, 1) and a tail with a characteristic exponential behavior (*red*, 2). (*C*) The exponential tail (*red*) is detected based on the recognition of the cutting point in (*B*). (*D*) The tail and the convolved decay are finally exploited to perform an ordinary deconvolution and estimate the IRF (*red dashed line*). The solid black line in (*D*) represents the true IRF.

MATERIAL AND METHODS

We examined various simulated and real data sets to evaluate the effectiveness of the proposed approach and the extraction of the IRF in TCSPC measurements. The simulated data sets were utilized to assess the algorithm performance under tightly controlled conditions, while the real data sets were employed to evaluate its potential in practical experimental scenarios.

Simulated data sets

Three distinct IRFs were generated with shapes resembling those commonly observed in TRFS experiments: the first IRF is a Gaussian function, the second is a sum of two overlapping Gaussian functions, and the third is a sum of three overlapping Gaussian functions (refer to Fig. S3). The underlying signal *x* was simulated as a monoexponential decay with a lifetime of 1 ns, utilizing 1500 time bins and a time resolution of 25 ps. Subsequently, *x* was convolved with the respective IRFs, resulting in three data sets: data set 1, data set 2, and data set 3 for the first, second, and third IRF, respectively.

To emulate real conditions, different levels of Poisson noise (no noise, a low level of noise representing 0.5% of the total variance, and a high level of noise representing 2% of the total variance) were introduced to the convolved signal. This comprehensive approach allowed us to thoroughly assess the performance of the proposed method under various conditions.

Experimental data sets

A solution of the commercial dye Alexa 647 (Thermo Fisher Scientific, Invitrogen) in PBS at pH 7.4 with a concentration of 5×10^{-7} M was prepared. Measurements was performed using a PicoQuant TCSPC system, equipped with a FluoTime 200 spectrometer (bandpass 4 nm, 90° and magic angle configuration) and a picosecond laser diode emitting at 640 nm, with a repetition rate of 8 MHz. Detection was performed using a microchannel plate photomultiplier tube (MCP-PMT, Hamamatsu, Germany) (PicoHARP300) with a bin time of 4 ps.

Measurements were conducted at three different power intensity (40, 50, and 80% for data sets 1, 2, and 3, respectively), with 10 replicates per power. The IRF was determined at the laser emission wavelength using the scattering of the laser from a nonfluorescent scattering solution (LUDOX colloidal silica solution). The full-width at half maximum of the IRFs was approximately 100 ps but very different shapes were observed for the different power intensities. The measurements were carried out for an emission wavelength of 660 nm (4 nm bandpass) and stopped when the number of counts reached a maximum value of 10,000.

Blind instrument response function identification (BIRFI) algorithm

BIRFI is designed to estimate the IRF solely from the analysis of the measured signal *y*. The methodology builds upon the properties of monoexponentially decaying functions when convolved, which guarantee that the lifetime of *x* is the same as the one determining the behavior of the tail of *y* (Eq. 1). By leveraging this property, the IRF can be readily extracted from the sole measurement of *y* as the solution of a system identification problem.

To elucidate how we can detect the monoexponential tail of *y*, consider the example depicted in Fig. 1. In this illustration, the signal *y* results from the convolution of a given IRF with a monoexponential *x* (refer to Fig. 1 *A*). Calculating the derivative of *y*, for instance, using the Savitzky-Golay algorithm (17), produces a profile with two distinctive trends in two different time intervals (see supporting material for additional details about the properties of this derivative profile): the first (interval 1 in Fig. 1 *B*) is associated with the region where the IRF significantly influences the shape of
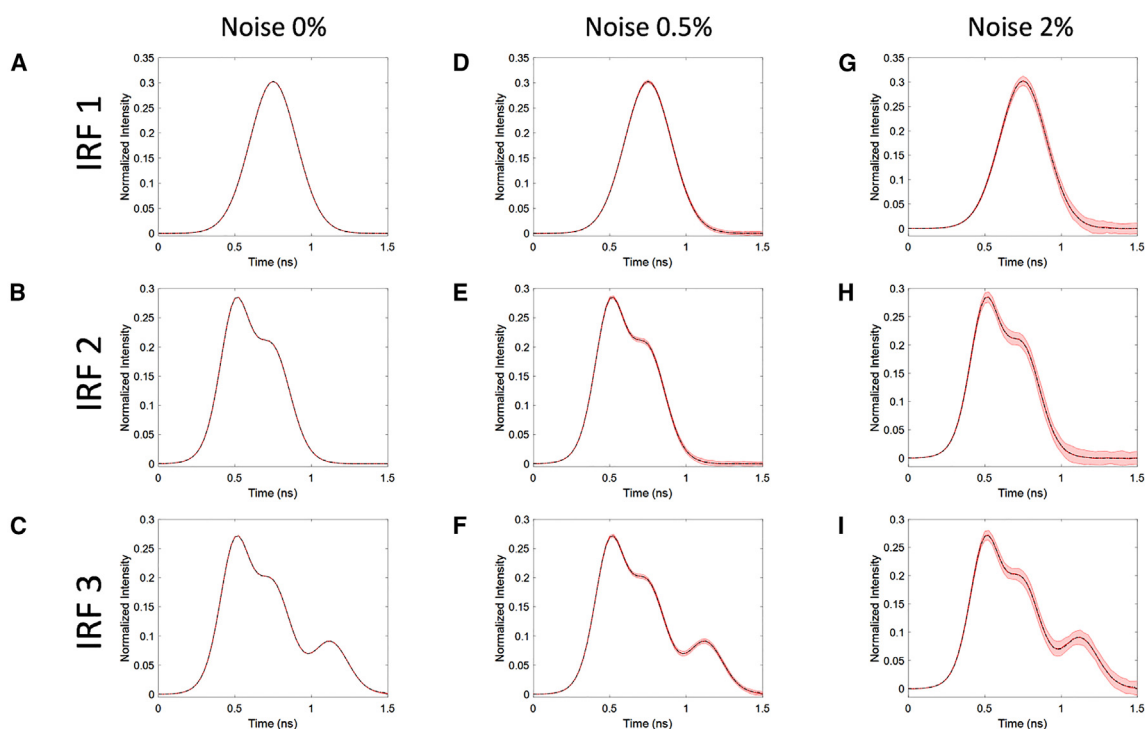
FIGURE 2 Predicted IRFs for three different levels of noise and three different expected IRF shapes. (*A–C*) Results of BIRFI in the absence of noise for three expected IRFs of different shapes. (*D–F*) Results of BIRFI in the presence of noise with intensity equal to the 0.5% of the total signal intensity for three expected IRFs of different shapes. (*G* and *I*) Results of BIRFI in the presence of noise with intensity equal to the 2% of the total signal intensity for three expected IRFs of different shapes. Each analysis round was repeated 100 times: the average predicted IRF is represented as a red solid line, the red shaded area denotes the 95% confidence interval associated to this average estimation, while the expected IRF is represented as a black dashed line.

y, and the second (interval 2 in Fig. 1 *B*) corresponds to the region where the derivative of *y* exhibits monoexponential behavior. The time point that separates these two regions is referred to as the "cutting point," and it can be easily observed through visual inspection in Fig. 1 *B*.

Here, three crucial points arise: first, computing the derivative of the measured signal facilitates the identification of the tail of *y*. Second, beyond the cutting point, *y* and *x* exhibit identical single exponential shapes but differ in amplitude (as illustrated by the *red line* in Fig. 1 *C*), and, third, the nonexponential part of *y* (Fig. 1 *C*, *black arrows*) has the same timespan of the IRF—for a rigorous mathematical explanation of this property, please refer to the supporting material.

At this juncture, with both *y* and *x* available (*x* being the tail of *y*), the blind identification problem and Eq. 1 transforms into a well-posed problem and estimating the IRF can be accomplished through ordinary long polynomial division, least-squares, or Fourier transform division.

Several noteworthy advantages afforded by the proposed methodology warrant emphasis. Foremost is the ability to retrieve the IRF by analyzing conventional fluorophores characterized by single exponential behaviors. Deconvolution is thus no longer impeded by emission wavelength dependencies since the deconvolved IRF is extracted directly from the measured signal and there is no need to use complex fluorophores with very short lifetimes which operate at specific wavelength, or to employ detectors robust to color effects. In addition, no assumption is made about the shape of the IRF, and no parameter optimization operations are required.

A pivotal aspect of BIRFI lies in its capability to reliably, automatically identify and extract the tail of *y* that decays exponentially as the inherent fluorescence signal *x*. Therefore, it is valuable not only for applying system identification procedures but also for tail analysis or global fitting, both of which necessitate isolating the tail of the measured signal.

However, it is essential to acknowledge some inherent limitations of the BIRFI method. Firstly, BIRFI assumes that the signal *x* is well approximated by a monoexponential decay function. In the rare scenarios where this requirement cannot be met by using very conventional fluorophores, blind unmixing tools should be applied to decompose *y* into its latent monoexponential decays before utilizing BIRFI to extract the IRF from such individual single exponential decays. To illustrate this, we provide as supporting material results obtained coupling a novel multivariate curve resolution approach named MCR-Slicing (18,19) to BIRFI in a case concerning multiexponential decaying signals.

In addition, it is crucial to highlight that since BIRFI extracts the IRF from the experimental measurement acquired, a sufficiently high signal-to-noise ratio in *y* is essential for accurate deconvolution. To mitigate noise effects, one may consider increasing photon accumulation during TRFS experiments or applying noise-filtering approaches like Savitzky-Golay (17) or Whittaker smoothing (20), as demonstrated in this work.

Software

Data simulation and analysis were performed by means of in-house routines and scripts coded in MATLAB 2021 (The MathWorks, Natick, MA). The BIRFI algorithm is explained in the supporting material. The DecayFit—time-resolved emission decay analysis
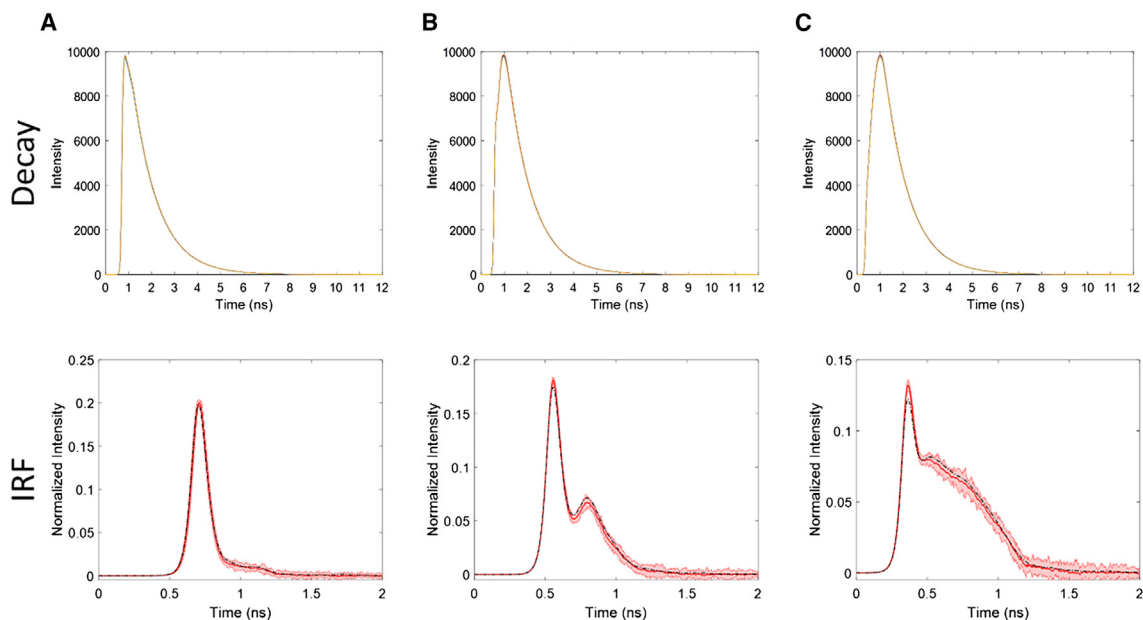
FIGURE 3 Results yielded by BIRFI for the first (*A*), second (*B*), and third (*C*) pure fluorescent dye data set. Top panel: smoothed fluorescence decays (10 replicates per case). Bottom panel: average predicted IRFs (*red solid lines*) three standard deviation intervals (*red shaded areas*), and measured IRFs (*black dashed lines*).

software for MATLAB (version 1.4, Søren Preus, PhD)—was used to perform the reconvolution analysis.

RESULTS AND DISCUSSION

Simulated data sets

To evaluate the performance of BIRFI, we delved into nine distinct data analysis scenarios, each distinguished by varying complexities in the shape of the RF and different levels of Poisson noise (refer to the supporting material for comprehensive details). Whittaker smoothing was systematically applied to all analyzed decays to mitigate the influence of noise. Decay curves for each scenario were replicated 100 times to scrutinize the variability of the solutions obtained due to noise. Notably, in all instances, the single exponential tail of the decays was successfully retrieved, as elaborated in the previous section. The conclusive results of these analyses are presented in Fig. 2.

Initially, in the absence of noise (refer to Fig. 2, *A−C*), as anticipated, the recovery of all IRFs is flawless, indicative of a well-posed signal identification problem.

Introducing noise into the scenario (see Fig. 2, *D−I*) reveals a minor dispersion in the recovered IRFs across the 100 replicated analysis rounds. Notably, the mean representation across these runs (depicted by the *red solid line*) impeccably aligns with the ground

truth (indicated by the *black dashed line*) in all instances. This alignment underscores that the observed dispersion is solely a result of the introduced noise and emphatically establishes the method accuracy.

These findings affirm that the methodology adeptly derives reliable estimates of the IRF from measured signals, operating without any prior assumptions about its shape.

Real data sets

To assess the performance of BIRFI on real experimental data, we conducted a series of TCSPC experiments. We analyzed ten replicates of TCSPC measurements conducted at three laser powers using a commercial Alexa 647 solution with a lifetime of 3.55 ns. Once again, Whittaker smoothing was applied as a preliminary step to each recorded decay, and the cutting point was set at 2.00 ns.

Fig. 3 illustrates the preprocessed data and the IRFs obtained through the application of BIRFI (depicted by the *red solid lines*). These results showcase a highly satisfactory agreement between the estimated IRFs and the measured ones (indicated by the *black dashed lines*). Minor discrepancies, possibly stemming from solvent effects, are the only observable differences.

To further validate the BIRFI approach and underscore its utility, we employed a parametric model (reconvolution) for each measured signal. This fitting
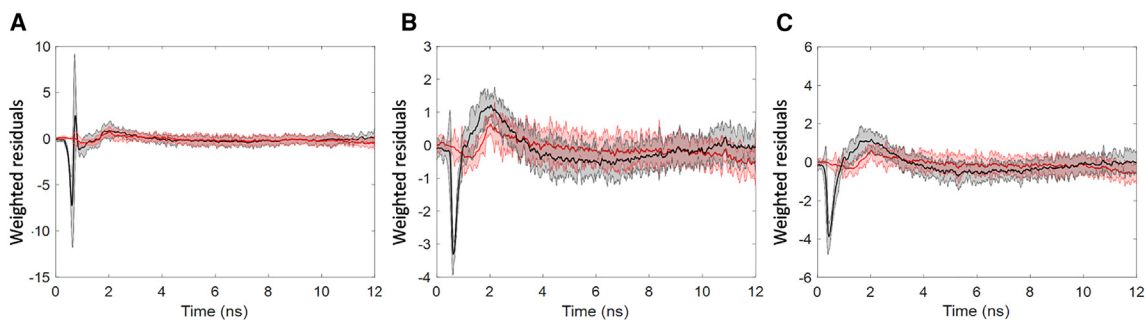
FIGURE 4 Weighted residuals resulting from the monoexponential fitting of the fluorescence decays in the first (*A*), second (*B*), and third (*C*) pure fluorescent dye data set. The fitting was performed with reconvolution using the IRF estimated by BIRFI (*red*) and the measured IRF (*black*). Each measurement replicate was fitted individually: the solid lines represent the average residual profiles, while the red and black shaded areas denote the corresponding three standard deviation intervals.

process involved utilizing both 1) the actual measured IRF and 2) the IRF estimated with BIRFI. The residuals of the parametric model are depicted in Fig. 4.

Moreover, the estimates of lifetimes were examined. In data set 1, a mean lifetime of 1.09(0.01) ns was derived using the predicted IRF, while a slightly lower estimate of 1.07(0.01) ns was obtained using the measured IRF. For comprehensive analysis, considering only the tail of the measured signal and fitting it with a monoexponential function yielded a mean lifetime of 1.09(0.01) ns. Although the lifetimes obtained in both cases are quite similar, the fitting residuals are notably less structured when reconvolution is performed with the IRF estimated through BIRFI compared with using the measured IRF (refer to Fig. 4 *A*).

Similar conclusions can be drawn for data sets 2 and 3. In data set 2, the average lifetimes are 1.07(0.01) and 1.04(0.01) ns when reconvolution is conducted using the IRF estimated by BIRFI and the measured IRF, respectively, while tail fitting provides a lifetime estimate of 1.08(0.01) ns. For data set 3, the average lifetimes are 1.08(0.02) and 1.05(0.02) ns, respectively, while tail fitting provides a lifetime estimate of 1.08(0.01) ns. In both cases, the fitting residuals obtained when reconvolution is carried out with the IRF estimated by BIRFI are significantly less structured (refer to Fig. 4, *B* and *C*).

Overall, these results indicate that utilizing IRFs estimated by BIRFI for fitting TRFS data collected on individual fluorophore solutions (via reconvolution) results in lower and less structured residuals compared with when measured IRFs are employed. This implies that better estimates of the fluorescence lifetimes of the species underlying the investigated systems may be achieved by employing BIRFI before TRFS data processing. Furthermore, considering residual analysis as a tool for assessing the validity of statistical models in the realm of TRFS, another critical point emerges from the presented outcomes: high residuals may arise not only from inadequately formulated models but also from poorly estimated or inaccurately measured IRFs. TRFS users should thus be attentive when attempting to address high residuals by introducing more complex models with a higher number of parameters.

CONCLUSIONS

In this communication, we introduced a novel method, called BIRFI, that enables the estimation of the IRF inherent in TRFS measurements, relying solely on the measurement of an exponential decay. This straightforward approach is grounded in the theoretical principles of convolution/deconvolution applied to monoexponential decays. As demonstrated, it possesses broad applicability, considering additional practical aspects that were also explored. Overall, BIRFI consistently delivered accurate estimates of the IRF across scenarios of varying complexity in terms of IRF shape, thus improving the accuracy of lifetime determination. Its robustness is now open to scrutiny and validation by potential users. Specifically, we believe that the application of BIRFI in experiments utilizing two-photon excitation, where emission occurs at a shorter wavelength than excitation, and conventional methods relying on scattering for IRF determination may not be applicable, will be of great interest for the community.

SUPPORTING MATERIAL

Supplemental information can be found online at https://doi.org/10.1016/j.bpr.2024.100155.

AUTHOR CONTRIBUTIONS

ACKNOWLEDGMENTS

DECLARATION OF INTERESTS

The authors declare no competing interests.

REFERENCES

1. Liput, D. J., T. A. Nguyen, …, S. S. Vogel. 2020. A guide to fluorescence lifetime microscopy and Förster's Resonance Energy Transfer in Neuroscience. *Curr. Protoc. Neurosci.* 94:e108.

2. Lakowicz, J. R. 2006. Principles of Fluorescence Spectroscopy, 3rd ed. Springer, USA.

3. Luchowski, R., Z. Gryczynski, …, I. Gryczynski. 2009. Instrument response standard in time-resolved fluorescence. *Rev. Sci. Instrum.* 80, 033109.

4. Riad, S. M. 1986. The deconvolution problem: An overview. *Proc. IEEE.* 74:82–85.

5. Abed-Meraim, K., W. Qiu, and Y. Hua. 1997. Blind system identification. *Proc. IEEE.* 85:1310–1322.

6. Szabelski, M., D. Ilijev, …, I. Gryczynski. 2009. Collisional quenching of erythrosine B as a potential reference dye for impulse response function evaluation. *Appl. Spectrosc.* 63:363–368.

7. Szabelski, M., R. Luchowski, …, I. Gryczynski. 2009. Evaluation of instrument response functions for lifetime imaging detectors using quenched Rose Bengal solutions. *Chem. Phys. Lett.* 471:153–159.

8. Bini, D., and V. Pan. 1986. Polynomial division and its computational complexity. *J. Complex.* 2:179–203.

9. Vetterling, W. T., S. A. Teukolsky, …, B. P. Flannery. 1999. Numerical Recipes in C: The Art of Scientific Computing. Cambridge University Press.

10. O'Connor, D. V., W. R. Ware, and J. C. Andre. 1979. Deconvolution of fluorescence decay curves. A critical comparison of techniques. Journal of *Physical Chemistry*. *J. Phys. Chem.* 83:1333–1343.

11. Xiao, D., N. Sapermsap, …, D. D. U. Li. 2021. On synthetic instrument response functions of time-correlated single-photon counting-based fluorescence lifetime imaging analysis. *Front. Physiol.* 9, 635645.

12. Wahl, P., J. C. Auchet, and B. Donzel. 1974. The wavelength dependence of the response of a pulse fluorometer using the single photoelectron counting method. *Rev. Sci. Instrum.* 45:28–32.

13. Reja, S. I., M. Minoshima, …, K. Kikuchi. 2020. Near-infrared fluorescent probes: a next-generation tool for protein-labeling applications. *Chem. Sci.* 12:3437–3447.

14. Ranjit, S., L. Malacrida, …, E. Gratton. 2018. Fit-free analysis of fluorescence lifetime imaging data using the phasor approach. *Nat. Protoc.* 13:1979–2004.

15. Štefl, M., N. G. James, …, D. M. Jameson. 2011. Applications of phasors to in vitro time-resolved fluorescence measurements. *Anal. Biochem.* 410:62–69.

16. Eilers, P. H. C., and C. Ruckebusch. 2022. Fast and simple super-resolution with single images. *Sci. Rep.* 12, 11241.

17. Savitzky, A., and M. J. E. Golay. 1964. Smoothing and differentiation of data by simplified least squares procedures. *Anal. Chem.* 36:1627–1639.

18. Devos, O., M. Ghaffari, …, C. Ruckebusch. 2021. Multivariate curve resolution slicing of multiexponential time-resolved spectroscopy fluorescence data. *Anal. Chem.* 93:12504–12513.

19. Gómez-Sánchez, A., M. Marro, …, A. de Juan. 2020. 3D and 4D image fusion: Coping with differences in spectroscopic modes among hyperspectral images. *Anal. Chem.* 92:9591–9602.

20. Eilers, P. H. C. 2003. A perfect smoother. *Anal. Chem.* 75:3631–3636.